The 9th European Congress on Computational Methods in Applied Sciences and Engineering
ECCOMAS Congress 2024
3–7 June 2024, Lisboa, Portugal

INVESTIGATION OF LENGTH SCALE DEFINITION INFLUENCE IN LES MODELS

E.Di Lavore , J.Ruano, A.Oliva and F.X.Trias

Heat and Mass Transfer Technological Center, Technical University of Catalonia, C/Colom 11, 08222 Terrassa (Barcelona), enrico.di.lavore@upc.edu

Key words: LES, length-scale, mesh anisotropy, OpenFOAM

Summary.

Large Eddy Simulations (LES) have been increasing popularity due to the decrease of computational power cost. Indeed, engineering applications which have previously involved mainly RANS, are now shifting to LES. Many eddy-viscosity models have been developed during the last decades. They all share a general structure, which derive from a dimensional analysis: $\nu_{SGS} = (C_m\Delta)^2 D(\bar{U})$, where in order appear the model constant, the length scale and the differential operator underlying the model. The aim of this paper is to investigate the influence of length scale Δ definition on highly anisotropic grids, because most of the research has focused mainly on the model constant and differential operator roles. The main length scale definitions that will be compared are: i) the most popular is $\Delta_{vol} = V^{\frac{1}{3}}$ ii) Δ_ω iii) Δ_{lsq}. In order to do so, we first calibrate the model constant, then we carry out a set of simulations in OpenFOAM to assess the Δ definition influence. In order to assess the resilience of the models for highly anisotropic meshes, these simulations will be carried out also on meshes having control volumes with high aspect ratios. Results for standard test cases such as a decaying Homogeneous Isotropic Turbulence (HIT) and a turbulent periodic plane channel will be presented and compared to reference cases.

1 INTRODUCTION

LES equations are obtained by applying a spatial filter to the Navier-Stokes equations. Usually a simple "box filter" is used, though more complex kernels can be used. This results in:

$$\begin{cases} \partial_t \bar{u} + (\bar{u} \cdot \nabla)\bar{u} = \nu \nabla^2 \bar{u} - \nabla \bar{p} - \nabla \cdot \tau \\ \nabla \cdot \bar{u} = 0 \end{cases}$$

In order to model the effects of turbulence acting on scales smaller than the filter length Δ , a eddy-viscosity model (e.g. WALE [7], Vreman's[9], QR[12], Sigma[11], S3PQR [16]) is usually applied, where the sub-grid scale viscosity is defined as $\nu_{SGS} = (C_m\Delta)^2 D(\bar{U})$. This is possible because the smallest resolved-scales motions provide information that can be used to model the largest SGS motions [5] . The aim of this paper is to verify the behavior of an eddy-viscosity turbulence model while different length-scale definitions are used on progressively higherly anisotropic meshes.

1.1 Length-scale definitions

In the LES community, the far more used mesh characteristic length-scale definition is the cubic root of the volume Δ_{vol} , introduced from Deardorff in 1970 [2]. Though, its performance is affected from a high aspect-ratio of the volumes, as in unstructured or highly anisotropic structured meshes. Indeed, this cause the model to be deactivated while the volume shrinks along one direction. In this situation, defining an optimal Δ it's not a trivial task. Nevertheless, in the DES community, a wider range of Δ 's definitions have been settled, to overcome different kinds of issues, for example taking into account flow and mesh anisotropy interaction for Δ_{ω} .

Two Δ definitions are identified for bounding others Δ behavior: Δ_{max} and Δ_{min} . Indeed, while refining the mesh in one direction, Δ_{max} is not affected at all, and Δ_{min} is progressively deactivating the model.

Among the others, Δ_{ω} [10] is meant to progressively deactivate the model while the mesh is refined in either direction of each plane normal to the vorticity versor. This because the in-plane velocity components associated to their vorticity component are acting in a progressively finer mesh, hence making the LES model progressively less necessary in that plane. Instead, Δ_{lsq} [17] it's based on a Taylor series approximation of the gradient model. The latter is characterized by keeping the influence of Δ as three separate components, in the form of diagonal of a tensor.

In the next section, the HIT case setup will be presented. Then the results in the form of energy density spectra will compared for different models and degrees of anisotropies. It will follow the Periodic Plane Channel case, where average velocities and Reynolds stresses will be plotted. Finally, some concluding remarks to summarise the Δ definitions behaviors.

2 TEST CASES

2.1 HIT

The first test case is the Homogeneous Isotropic Turbulence (HIT) decay in a periodic cube. For this case we have used as reference the results from the historical paper by Comte-Bellot and Corrsin (CBC) [3].

The comparison between the time-evolving HIT and the spatial decay of stationary turbulence in a wind-tunnel, it's relying on Taylor's hypothesis. This latter leads to the assumption that the spatial correlations of the turbulent velocity components correspond well enough to their self-correlations in time i.e. (using CBC notation) $R_{11}(r, 0, 0; t_0, 0) \approx R_{11}(0, 0, 0; t_0, r/\bar{U})$, which have been verified from Favre et alia [1].

The non-dimensionalization procedure preserves the Taylor micro-scale Reynolds number $\mathrm{Re}_{\lambda} = \frac{u_{rms} \cdot \lambda}{\nu} = 71.6$, with a cubic box side length $L_{box} = 0.09 \cdot 2\pi$, a $u_{rms} = 0.222$ and a viscosity $\nu = 10^{-5}$.

The mesh anisotropy is increased by progressively refining the mesh along z-axis. We started with a uniform mesh of 64^3 volumes, with the following mesh refinement: $64 \times 64 \times N_z$ with $N_z \in \{64, 128, 256, 512, 1024\}$.

Regarding the turbulence model, we have chosen Smagorinsky for its simplicity, due to the absence of walls in this case; whereas for the time integration, a backward 2^{nd}order explicit Euler is used , with a constant $\Delta t = 10^{-3}$.

HIT Results

The resolved kinetic energy density spectrum are computed at dimensionless times $tU_0/M = 42\,;\,98\,;\,171$ and compared with the results from CBC [3]. In Figure 1 are summarized the outcomes of the HIT case. In each plot is presented the temporal decay of the energy density spectra, where time correspondence is done by keeping the dimensionless similarity with the reference.

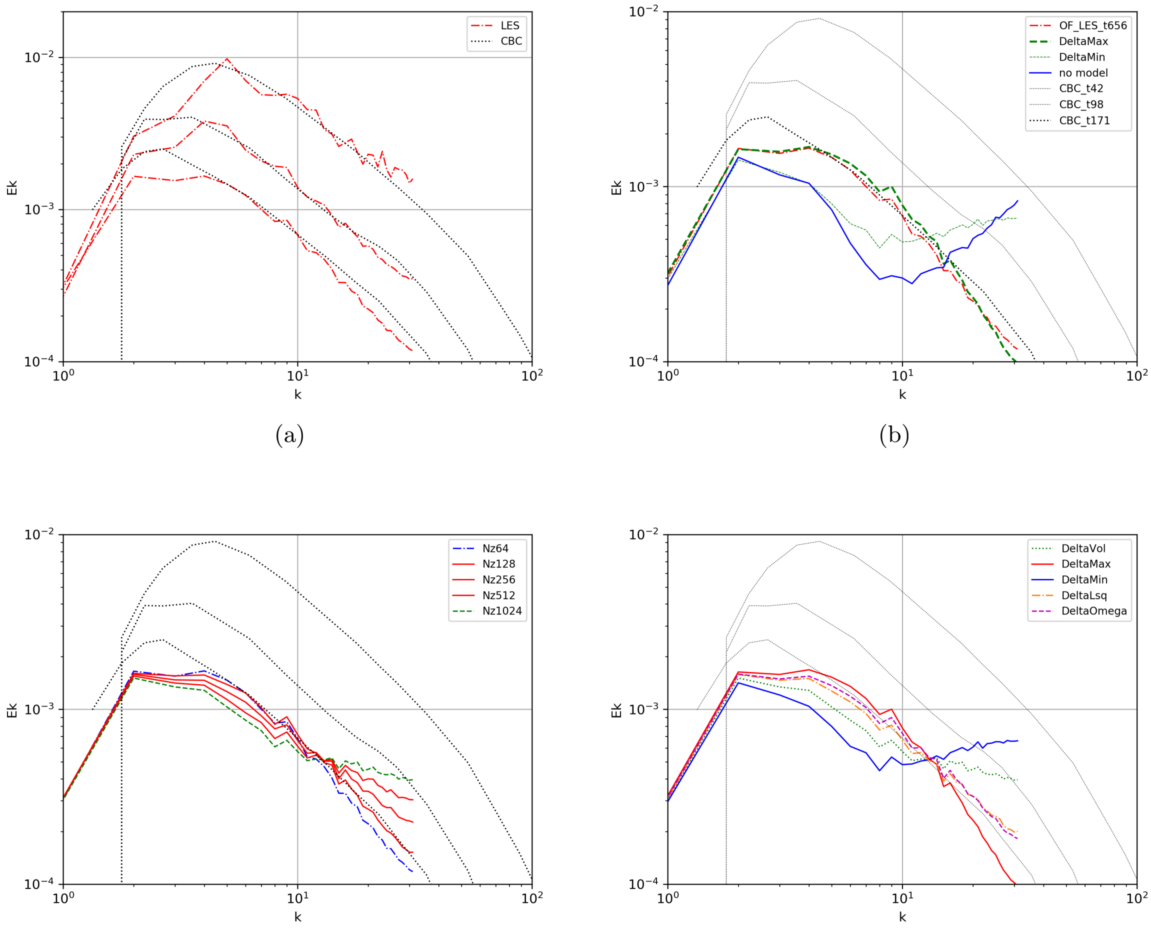

(a) (b) (c) (d)

Figure 1: Energy density spectra

In the plot 1(a) is illustrated the spectrum of the main case run in OpenFOAM i.e. on a isotropic mesh using Smagorinsky model with Δ_{vol}. A consistent energy loss in the energy-containing range can be noticed, but overall the Kolmogorov $\frac{5}{3}$ law is fulfilled in the inertial subrange. Anyway, the model produces results (red dash-dotted) in agreements with the reference (always represented as thinner black dotted) [3].

In the plot 1(b) , keeping the reference in the background, we still show the spectrum at the last of the considered time-steps, run on isotropic mesh with Δ_{vol} (red dash-dotted). Then we compare the latter, at first with the same case run without LES model (blue continuous) to verify that the model is acting properly by modelling the SGS scales and dissipating the non resolved modes. Indeed, ν_{sgs} is properly damping the turbulent kinetic energy pile-up that can be seen instead in the model-less case. We also show the Δ_{max} (thick green dashed) and Δ_{min} (thin green dashed) spectra from the most anisotropic case (64x64x1024). Intuitively, Δ_{min} is showing a dissipating behavior similar to the model-less case, because the z-axis grid spacing it's so small that is almost deactivating the model. Instead, all Δ 's behaves equally to the Δ_{vol} on isotropic mesh, because they are returning the same length-scale, hence same ν_{sgs}.

In the plot 1(c) we show the pencil of spectra generated by increasing the degree of anisotropy in the case of Δ_{vol}. Here the isotropic case spectrum (blue dash-dotted) and the highly anisotropic case spectrum with $N_z = 1024$ (green dashed) upper/lower bound the results: the isotropic case upper-bounds in the inertial subrange and lower-bounds in the dissipation range ; increasing anisotropy leads to an over dissipation in the inertial sub-range and an under-dissipation in the dissipation range due to the non realistic turbulence seen in the plot 1(b). This leads graphically to the pivoted pencil visible in plot 1(c).

Finally in plot 1(d) we do the most relevant comparison: are plotted the spectra of all the used models in the higly anisotropic case. We have already seen the behaviors of Δ_{min} and Δ_{max}, and here we see that they upper and lower bound the results of all the other length-scale definitions. Δ_{vol}, even if in a minor extent, still suffers model deactivation due to high anisotropy, because the volume is simply reduced by the refinement. The models that show to perform the best are Δ_{ω} and Δ_{lsq}, which substantially agree with the reference [3].

2.2 Periodic Plane Channel

The second test case is the periodic plane channel where the flow's turbulence developement is guaranteed by applying periodic boundary condition at stream-normal faces while the stationarity is enforced by a volume force in the stream-wise (x) direction. The reference for this case is the DNS from Kim, Moin and Moser [4] . We have used a channel size $(20\pi, 2, \pi)$. Viscosity is set in order to keep the viscous Reynolds number $\mathrm{Re}_{\tau} = 180$ as in the reference. Due to the wall-normal (y-axis) mesh inhomogeneity, we have refined the mesh in either stream-wise or span-wise directions. Wall-normal spacing have been kept the same as the initial mesh, which is a homogeneous 32^3 except along wall-normal direction, where a hyperbolic tangent mapping is applied to resolve the boundary layers. The meshes are respectively N_xx32x32 and 32x32xN_z with $N_x, N_z \in \{64, 128, 256, 512, 1024\}$.
For this case we have used the turbulence model WALE [7] that properly deactivates the model's effect close to the walls. For time integration, we have used a CFL-adaptive time-stepping, with $\mathrm{C}_{max} = 0.6$ on a 3^{rd} order Runge-Kutta scheme implemented in the solver RKsymFoam, which has implemented a symmetry-preserving spatial discretization. [8, 13, 18]

Periodic Plane Channel Results

In order to compare the run cases with the reference [4], we plot in both the homogeneous-ensemble average velocity and the Reynolds stresses.

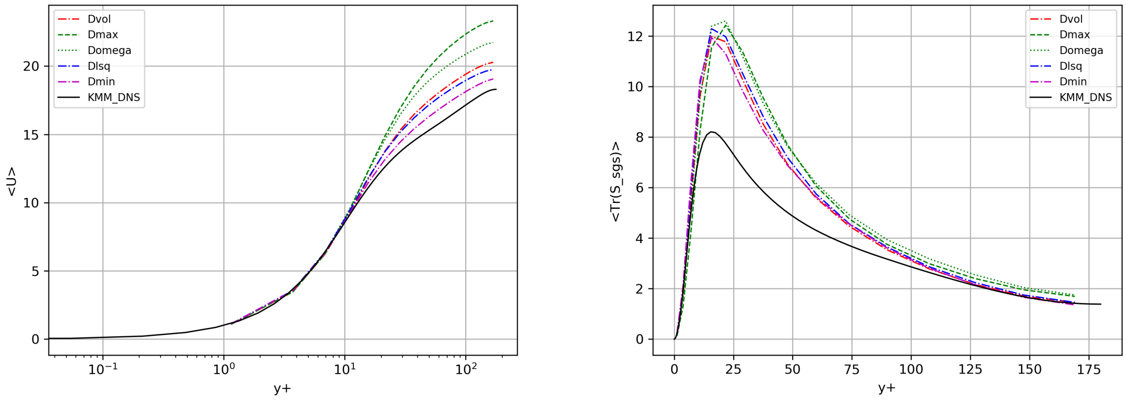

(a) (b)

Figure 2: Ensemble-average stream-wise velocity and trace of Reynolds stress tensor in 32^3 mesh

In figure 2 are shown the behaviors of different Δ definitions on the same 32^3 mesh (which is not isotropic due to the channel aspect ratio). Again, Δ_{max} and Δ_{min} are bounding the others Δ definitions. Anyway, it can be seen that even with Δ_{min} , the model is over-dissipating turbulence, which leads to a higher bulk velocity due to a lack of transport of momentum from the walls towards the central plane of the channel.

In figure 3 is shown how the mesh refinement along the x-axis have reduced this over-dissipation effect by reducing the pencil-shape volume's length such that the volume become a x-axis pancake-shape one. This is considered a natural behavior since in finer meshes, turbulence models become progressively less necessary, up to a resolution that allows for DNS.

Also, this refinement led all the Δ definitions to converge to the same average velocity profile, which still present an over-dissipation of turbulence, hence making this discrepancy independent of LES model.

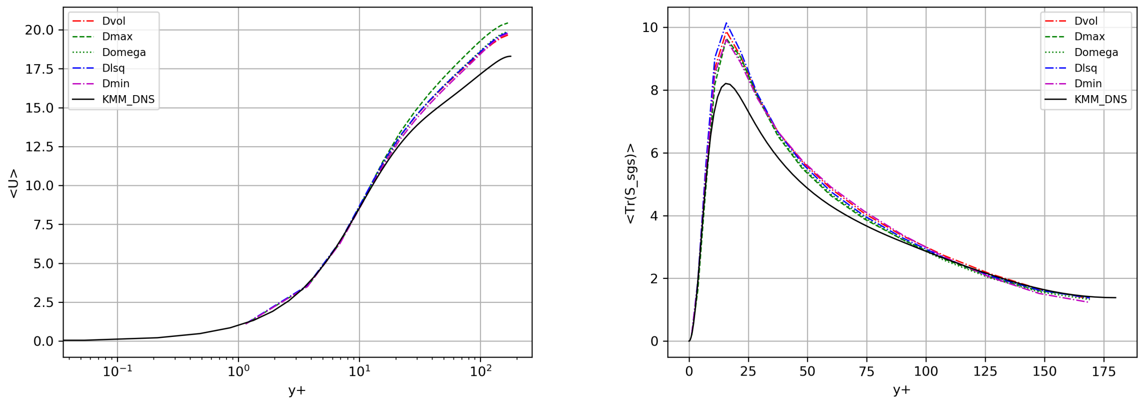

(a) (b)

Figure 3: Ensemble-average stream-wise velocity and trace of Reynolds stress tensor in $512x32x32$ mesh

As it can be seen in figure 4, the mesh refinement impact consistently the behavior of each Δ definition. We can see in plot 4(b) that the refinement makes Δ_ω to converge closer to the actual result, even if the limit curve it's still not the reference from [4]. Anyway, it shows an asymptotical behavior to a steady value. Instead, Δ_{vol} in plot 4(a) shows a less significant dependency on the mesh. Indeed the mesh refinement don't show a monotonic approach to a limit curve, but the curves' pencil shows a consistent behavior compared to the asymptotic value of Δ_ω . The Δ definition which is showing the most resilience to mesh anisotropy is the Δ_{lsq} [17], which results overlap while refining the mesh along x-axis.

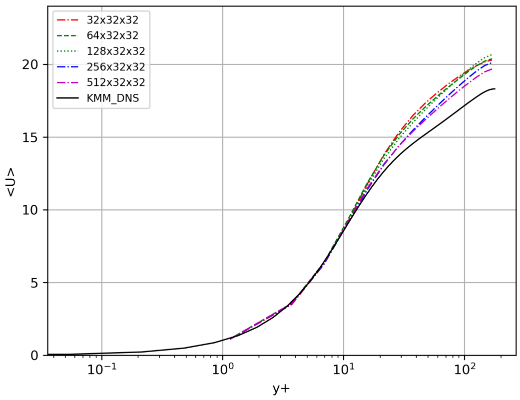

(a) Δ_{vol}

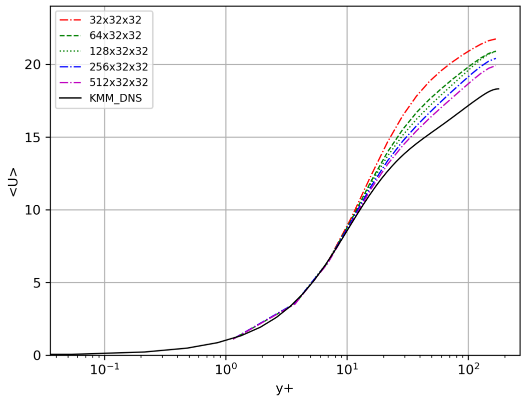

(b) Δ_{ω}

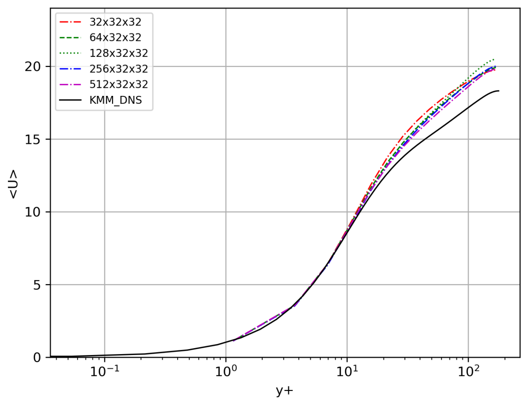

(c) Δ_{lsq}

Figure 4: Ensemble-average stream-wise velocity: length-scale definition influence on x-refinement

3 CONCLUSIONS

In this work we have tested different length-scale definitions on a range of mesh anisotropies in two cases, namely the HIT and the plane channel. We have seen how different Δ definitions have shown quite different resilience properties with respect to mesh refinement. In particular, Δ_{lsq} [17] have shown to be the least affected from the anisotropies among the tested length-scales, which is in line with the fact that it has been designed with this purpose. Further research can be done with other lenght-scale definitions as Δ_{SLA} [15], which is a modification of $\tilde{\Delta}_{\omega}$ [14] suited to trigger Kelvin-Helmoltz instability in the shear layer, or Δ_{Sco} [6] which is one of the corrections of Deardorff's Δ_{vol} [2] required for highly anisotropic meshes as for near wall turbulence and shear layers.

Acknowledgments. This work is supported by SIMEX project (PID2022-142174OBI00) of *Ministerio de Ciencia e Innovacion* and the RETOtwin project (PDC2021-120970-I00) of *Ministerio de Economia y Competitividad*, Spain. E.D.L is supported by Programa Investigo (2023 INV-2 00044) of the Catalan Agency for Management of University and Research Grants (AGAUR). Calculations were carried out on JFF2 computer cluster at CTTC. The authors thankfully acknowledge these institutions.

REFERENCES

[1] A.Favre, J.Gaviglio, R.Dumas, Appareils de mesures de la correlation dans le temps et l'espace. Quelques mesures de correlation dans le temps et l'espace en soderie. Proc. 8th Int. Gong. for Appl. Mech., Istanbul, 304-314, 314-324, 1952

[2] J. W. Deardorff, Numerical study of three-dimensional turbulent channel flow at large Reynolds numbers, J. Fluid Mech. 41, 453–480, 1970

[3] G. Comte-Bellot and S. Corrsin, Simple Eulerian time correlation of full- and narrow-band velocity signals in grid-generated, isotropic turbulence, J. Fluid Mech. 48, 273–337, 1971

[4] J. Kim, P. Moin, and R. D. Moser, Turbulence statistics in fully developed channel flow at low Reynolds number, J. Fluid Mech. 177, 133 , 1987

[5] Germano, M., Piomelli, U., Moin, P. and Cabot, W.H. , A dynamic subgrid-scale eddy viscosity model. Physics of Fluids A: Fluid Dynamics, 3(7), pp.1760-1765, 1991

[6] A. Scotti, C. Meneveau, and D. K. Lilly, Generalized Smagorinsky model for anisotropic grids, Phys. Fluids A 5(9), 2306–2308 , 1993

[7] Nicoud, F., Ducros, F. Subgrid-Scale Stress Modelling Based on the Square of the Velocity Gradient Tensor. Flow, Turbulence and Combustion 62, 183–200, 1999

[8] Verstappen, R.W.C.P. and Veldman, A.E.P., Symmetry-preserving discretization of turbulent flow, Journal of Computational Physics, 187(1), pp.343-368, 2003

[9] W. Vreman, An eddy-viscosity subgrid-scale model for turbulent shear flow: Algebraic theory and applications, Phys. Fluids 16(10), 3670–3681, 2004

[10] Deck, S. Recent improvements in the Zonal Detached Eddy Simulation (ZDES) formulation. Theor. Comput. Fluid Dyn. 26, 523–550, 2012

[11] Nicoud, Franck, Hubert Baya Toda, Olivier Cabrit, Sanjeeb Bose, and Jungil Lee, Using singular values to build a subgrid-scale model for large eddy simulations, Physics of fluids 23, no. 8, 2011

[12] R. Verstappen, When does eddy viscosity damp subfilter scales sufficiently?, J. Sci. Comput. 49(1), 94–110, 2011

[13] F. X. Trias, O. Lehmkuhl, A. Oliva, C. D. Perez-Segarra, R. W. Verstappen, Symmetry-preserving discretization of Navier–Stokes equations on collocated unstructured grids, Journal of Computational Physics 258 246–267, 2014

[14] C. Mockett, M. Fuchs, A. Garbaruk, M. Shur, P. Spalart, M. Strelets, F. Thiele, and A. Travin, Two non-zonal approaches to accelerate RANS to LES transition of free shear layers in DES, in Progress in Hybrid RANS-LES Modelling, Notes on Numerical Fluid Mechanics and Multidisciplinary Design Vol. 130, edited by S. Girimaji, W. Haase, S.H. Peng, and D. Schwamborn, pp. 187–201, 2015

[15] Shur, M.L., Spalart, P.R., Strelets, M.K. et al. An Enhanced Version of DES with Rapid Transition from RANS to LES in Separated Flows. Flow Turbulence Combust 95, 709–737, 2015

[16] Trias, F. X., David Folch, Andrei Gorobets, and A. Oliva, Building proper invariants for eddy-viscosity subgrid-scale models, Physics of Fluids 27, no. 6, 2015

[17] F.X.Trias, A.Gorobets, M.H.Silvis, R.W.C.P.Verstappen, A.Oliva. A new subgrid characteristic length for turbulence simulations on anisotropic grids. Physics of Fluids 29, 115109, 2017.

[18] E.M.J. Komen, J.A. Hopman, E.M.A. Frederix, F.X. Trias, R.W.C.P. Verstappen, A symmetry-preserving second-order time-accurate piso-based method Computers & Fluids, 225: 104979, 2021